

# Towards a New Approach in Designing High-Strength Concrete: Challenges in Replacing Three-Fourth of Natural Fine Aggregate with Coal Bottom Ash

Deepthi Shenoy, Sugandhini H. K., Laxman Kudva P.\*

Department of Civil Engineering, Manipal Institute of Technology, Manipal Academy of Higher Education, Manipal 576104, Karnataka, India

Received August 18, 2024; Revised November 11, 2024; Accepted December 11, 2024

## Cite This Paper in the Following Citation Styles

(a): [1] Deepthi Shenoy, Sugandhini H. K., Laxman Kudva P., "Towards a New Approach in Designing High-Strength Concrete: Challenges in Replacing Three-Fourth of Natural Fine Aggregate with Coal Bottom Ash," *Civil Engineering and Architecture*, Vol. 13, No. 1, pp. 522 - 542, 2025. DOI: 10.13189/cea.2025.130133.

(b): Deepthi Shenoy, Sugandhini H. K., Laxman Kudva P. (2025). Towards a New Approach in Designing High-Strength Concrete: Challenges in Replacing Three-Fourth of Natural Fine Aggregate with Coal Bottom Ash. *Civil Engineering and Architecture*, 13(1), 522 - 542. DOI: 10.13189/cea.2025.130133.

Copyright©2025 by authors, all rights reserved. Authors agree that this article remains permanently open access under the terms of the Creative Commons Attribution License 4.0 International License

**Abstract** Globally, thermal power plants produce about 780 million tonnes of coal ash, of which Asia alone accounts for 66% of this share. India, the third-largest coal ash producer, generated 226 million metric tonnes in 2019. Conserving natural resources and promoting viable alternatives are priorities that contribute to achieving sustainable development goals. This study aims to assess the fresh and hardened properties of high-strength concrete, in which 75% of natural fine aggregate (NFA) is supplemented with coal bottom ash (CBA). This study assessed ultrasonic pulse velocity and compressive strength at 3, 7, 28, 56, and 90 days using 100 mm cube specimens, split tensile and flexural strength at 7 and 28 days with 150 mm dia. × 300 mm height cylindrical specimens and 500×100×100 mm beam specimens, respectively. A minimum of three samples are tested in each group per test, and the average values are recorded. The findings reveal promising outcomes for using high-volume CBA as a feasible alternative to NFA. The concrete exhibited commendable early-age hardened properties with a 28-day compressive strength of 79.73 MPa, flexural strength of 7.2 MPa, and split tensile strength of 3.25 MPa, supporting the suitability of CBA in high-strength applications. The higher water absorption of CBA due to its porous structure may have led to a higher slump value. However, it's important to note that a higher slump value meant that the slump was a collapse pattern, and the mix also showed significant bleeding, segregation,

and a longer setting time, which presents a considerable challenge when attempting to incorporate higher volumes of CBA into concrete.

**Keywords** Coal Bottom Ash, Natural Fine Aggregate, High-Strength Concrete, Mechanical Properties, Sustainable Development Goals

---

## 1. Introduction

Concrete is a widely utilized material in the construction industry [1]. Developing countries like India are experiencing significant growth and expansion in infrastructure development, resulting in the growth of annual consumption of concrete and, thus, the consumption of cement and sand [1, 2]. This surge in demand has raised concerns about environmental pollution and depleting natural resources [3], with approximately 10% of CO<sub>2</sub> emissions expected to contribute to rising temperatures and climate changes [4]. Coarse and fine aggregates comprise approximately 60 to 70% of the total volume of concrete [5]. Gradual exhaustion of natural resources results in environmental degradation and a reduced supply of natural aggregates [5, 6]. As a result, identifying substitutes for natural aggregates is crucial to reducing the reliance on natural resources [1].

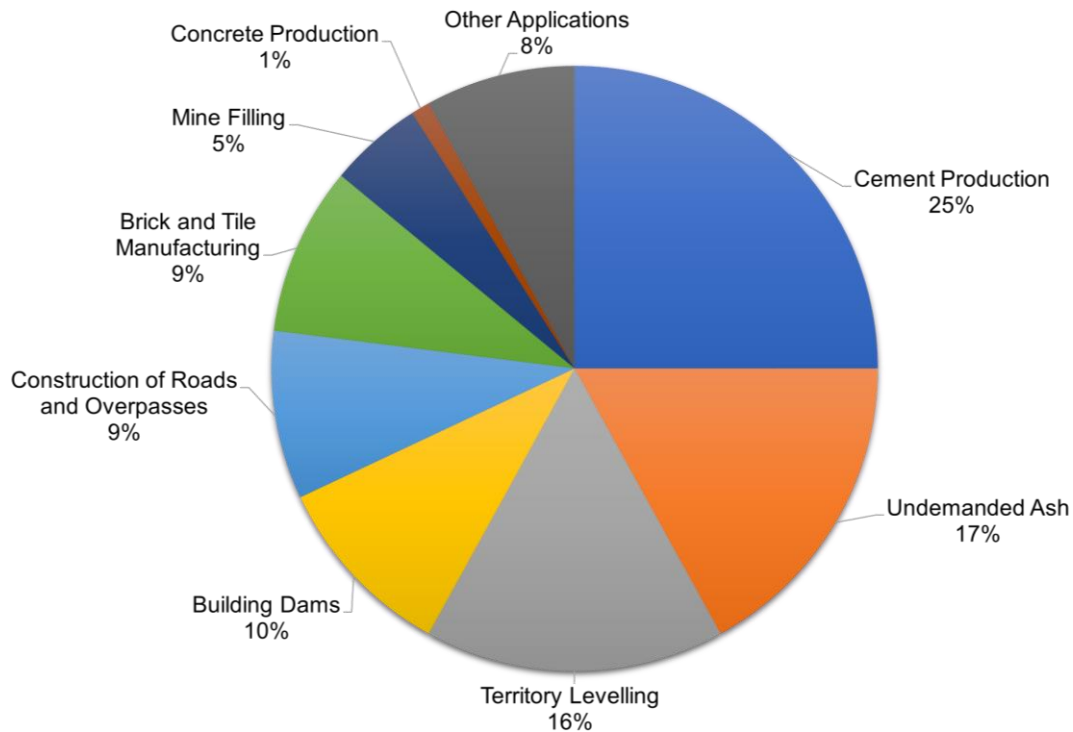


**Figure 1.** Categories of Coal Ash Utilization in India (adapted from [8])

Currently, industrial waste generation is a global issue [7]. Power plants are responsible for approximately 38% of global energy production, with India contributing over 65% of this share [1]. The combustion of coal in thermal power plants for global electricity generation has led to the production of coal ashes as byproducts. Around 150 to 200 million tonnes of bottom ash is produced worldwide, with Asia producing a substantial amount of CBA [8, 9]. The carbon emissions associated with cement consumption and production could be reduced by incorporating locally sourced byproducts in concrete production [10]. Replacing cement with industrial byproducts to improve its properties is a common approach to producing sustainable concrete [11]. However, the potential applications of CBA in concrete have not been investigated thoroughly. In India, approximately 173 million tonnes of coal ash are produced, of which 35 million tonnes of collected waste is CBA [12]. Figure 1 represents the categories of the utilization of coal ash in India.

In addition to the increasing concern of its generation, the disposal of CBA poses a significant concern due to expensive landfill sites and the hazards they cause [13]. The harmful constituents present in CBA raise concern, particularly with respect to ground and surface water contamination, thereby affecting public health [8, 13–15]. This necessitates developing approaches to manage the growth of CBA generation and protect the environment [12]. On a global scale, using around 50% of non-renewable resources has rendered the construction industry the least sustainable [16]. The construction sector provides a huge opportunity to utilize CBA in construction materials [12]. Over the last four decades, studies on its use

as a substitute for natural sand have gained significant attention [17]. It could be a potential application to provide a sustainable solution for the environmental hazards faced [5, 12, 18].

### 1.1. Utilization of CBA in Concrete

Several studies suggest CBA as a potential alternative to natural sand in concrete. The large particle size of CBA and the resemblance of particle size distribution to natural sand have led previous studies to consider CBA a potential substitute for fine sand in mortar and concrete [19–22]. Hasim et al. revealed a promising outcome that supports the suitability of high-volume CBA as a replacement for NFA and coarse aggregates (CA) in normal-strength concrete [23]. The optimal sand replacement levels in the literature were identified to be in the range of 30 to 45% for normal-strength concrete [24]. Despite its utilization in concrete as an alternative to sand, the relatively lower pozzolanic activity of CBA than materials like fly ash and rice husk ash and their larger porous particles hamper its utilization as cement replacement or in geopolymer applications [22, 25]. However, CBA exhibits high pozzolanic reactions and could serve as a potential alternative for cement in concrete on particle size reduction [7, 19].

Coal ash poses potential environmental hazards [14]. Therefore, this necessitates the examination of the environmental impacts of coal ashes before their utilization in any form, despite the uncertainties regarding their potential risks [9, 26]. Arsenic, mercury, lead, and cadmium are among the toxic constituents present in the

coal ashes obtained from some thermal power plants in India. CBA is not listed as hazardous in countries like China and the United States, primarily because of its potential industrial application [26]. On the other hand, countries like Malaysia, Singapore, and Thailand have classified CBA as hazardous [27]. Despite the potential of CBA to be utilized as fine aggregates, its implementation in structural concrete poses several challenges compared to using fly ash as a binder. The porous nature of CBA can raise concerns regarding the consistency, workability, and durability of the concrete [17].

### 1.2. Effect of CBA on Fresh and Hardened Properties of Concrete

The fresh properties of CBA concrete indicate inconsistent results when replaced with sand and cement to produce concrete. Several studies observed a declining workability trend when higher CBA contents are incorporated into the concrete mix [23, 28]. However, contrasting findings were reported regarding CBA utilization as OPC in mortar [14]. CBA mix generally exhibited better workability than a mortar with only cement and fly ash [29]. At a fixed water-to-cement ( $w/c$ ), bleeding showed a significant decrease when fine aggregates were entirely substituted with CBA. On the other hand, literature studies have also revealed that the presence of higher  $w/c$  led to prolonged bleeding with increasing CBA content [14].

CBA concrete mixes initially exhibited lower strength developments at an early age [24]. Several studies have demonstrated a significant impact of CBA on the compressive strength of concrete, reporting a wide range of compressive strength values when replaced as sand and cement in concrete [15, 25, 30, 31]. CBA replacement to sand demonstrated enhanced compressive strengths only at lower percentages of CBA content [15]. The general trend observed by most of the studies was a decline in compressive strength with increasing CBA substitution [15, 18, 23, 28, 32]. However, some studies [4] presented contrasting findings, showing increased strength with increasing aggregate replacement. Moreover, incorporating CBA at increasing levels in high-strength concrete (HSC) led to a marginal decrease in compressive strength, even though the compressive strength of mixes with complete substitution of CBA exceeded the target design strength [18]. Most of the studies identified 5 to 20% as the optimum replacement level for CBA without compromising the strength of concrete [25, 31].

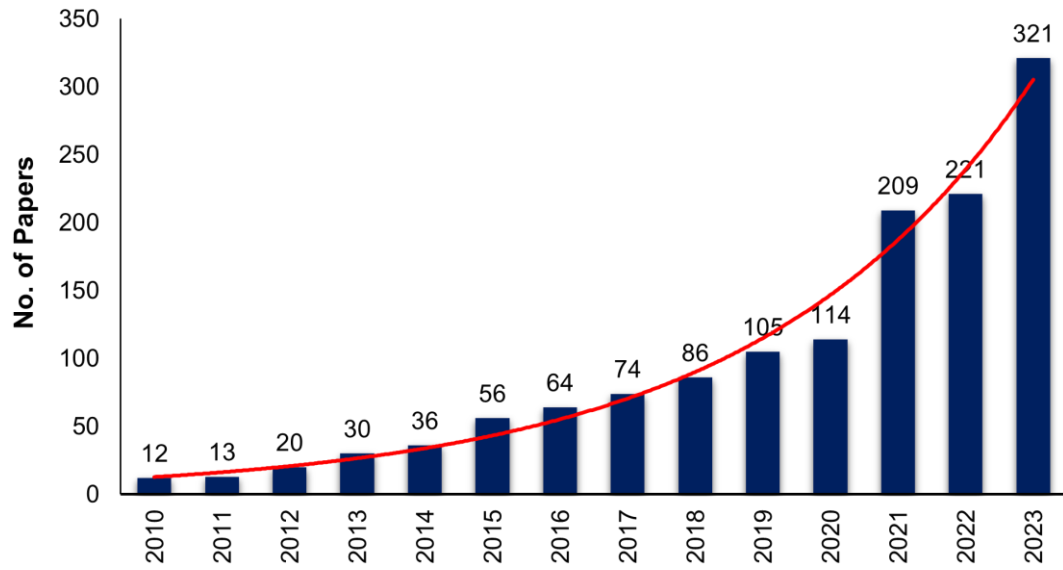
The split tensile and flexural strength observed in previous studies exhibited certain variations. Previous studies have generally observed a declining trend of

flexural and split tensile strengths with increasing levels of CBA substitutions to sand [14, 18, 19, 23, 30]. Studies have reported an increase [3] and a decrease in split tensile strength with increasing replacement levels of CBA in concrete [28, 32]. Mortar and concrete mix constituting 10 to 30% CBA followed an increasing trend of split tensile strengths, whereas, beyond 40% replacement levels, the split tensile strengths were observed to follow a declining trend [25]. However, Yang et al. demonstrated that CBA replacement to NFA had no significant impact on the split tensile strength of HSC at any replacement level [18]. Limited studies that evaluate the mechanical properties of concrete constituting CBA as cement replacement have been carried out. However, when replaced as a binder, the flexural strength of resulting mixes was initially comparable to that of control concrete for a lower replacement level, following a reduction with increasing CBA content [31].

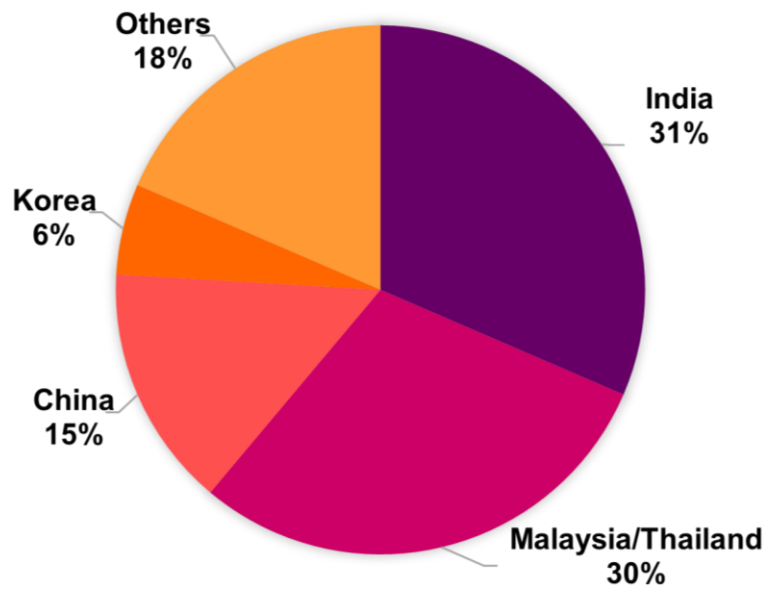
### 1.3. Significance of the Study

The literature review highlights significant research on utilizing CBA as a substitute for NFA and cement in concrete. Figure 2 illustrates a bibliometric analysis of a decade of subject-related publications from the Scopus database. Significant research has focused on exploring the potential of CBA as NFA in concrete production. However, the statistical analysis of available studies reveal a predominant focus on CBA's application in normal-strength concrete, highlighting a major limitation in its exploration of high-strength concrete (HSC). Moreover, most of the research reviewed in this study concerning HSC adheres to Korean standards. In contrast, studies within the Indian context predominantly pertain to normal-strength concrete. Furthermore, existing studies on HSC indicate an optimal CBA replacement level in concrete ranging from 45% to 60%, as illustrated in Figure 3. Therefore, this study aims to investigate the feasibility of utilizing high-volume CBA (HVCBA) at a 75% replacement rate in HSC, focusing on the fresh and mechanical properties of concrete.

This study introduces several novel aspects of the development of HSC. It employs a ternary blend of OPC, fly ash, and silica fumes with coarse and fine CBA as a substitute for natural sand in concrete, with a low water-to-cementitious material ( $w/c_m$ ) ratio to enhance the material properties. This study also explores the potential of replacing natural sand with HVCBA (75%), achieving compressive strength values within the HSC grade. The practical challenges concerning workability are also discussed, and the relevant factors are collated, offering critical insights to assist future research on optimizing concrete mixes with similar compositions.



(a)



(b)

**Figure 2.** (a) Year-wise publication of subject-related papers in Scopus (Note: This figure represents publication trends for years 2010-2023 and is based on the Scopus database, papers searched using keywords 'coal bottom ash', 'high-strength concrete' and (b) Statistics of literature reviewed for the present study

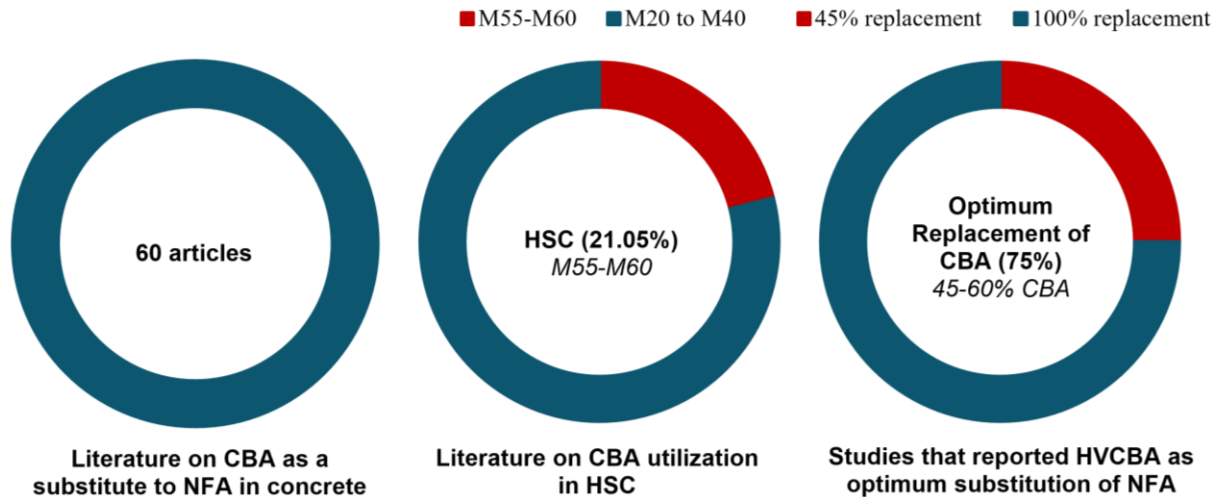


Figure 3. Statistical analysis of the literature reviewed in the present study

## 2. Materials and Methodology

Figure 4 illustrates the methodology of the study. The present study utilizes OPC grade 53, conforming to IS 269-2015 [33], fly ash conforming to IS 1727-1967 [34], microsilica as binders, and CA and NFA conforming to IS 383-2016 [35] and CBA as fillers. A polycarboxylate ether (PCE) based superplasticizer is used to achieve a low  $w/c_m$  ratio. The CA used were 16 mm and 12.5 mm crushed natural granite, and sand was used as NFA. Figure 5 illustrates the particle size distribution of CA, NFA, and CBA, and Table 1 and Table 2 present the physical properties and chemical composition of the materials, respectively.

### 2.1. Mix Proportion

The concrete mixes were designed for a characteristic strength of 65 MPa as per IS 10262-2019 [47] for a fixed  $w/c_m$  ratio of 0.29. CBA concrete incorporated 75% CBA by weight, with fixed binder and CA content. PCE-based superplasticizer was introduced at 0.8% by weight of binders. Table 3 presents detailed mix proportions. The

concrete mixes were designed based on SSD conditions, and necessary corrections were made to the water requirements while batching.

### 2.2. Particle Packing Model

This study utilizes the Modified Andreasen particle packing model to evaluate the particle arrangement in the mix, optimized with the Elkem Materials Mixture Analyser (EMMA) software, adopting a distribution modulus of 0.26. The ideal curve is attained with particle sizes ranging from 10 microns to 16 mm. The curves resulting from 0 and 75% replacement of NFA with CBA are then compared to the ideal curve for optimal packing. Figure 6 represents the particle packing curves obtained from EMMA software for control and CBA concrete. The results indicate that the mix with 75% CBA contains more fines than the control mix. Although the control mix shows better particle packing, increasing the coarser fractions could further improve it. Similarly, increasing coarser fractions and reducing finer fractions in CBA75 concrete could further enhance the particle packing.

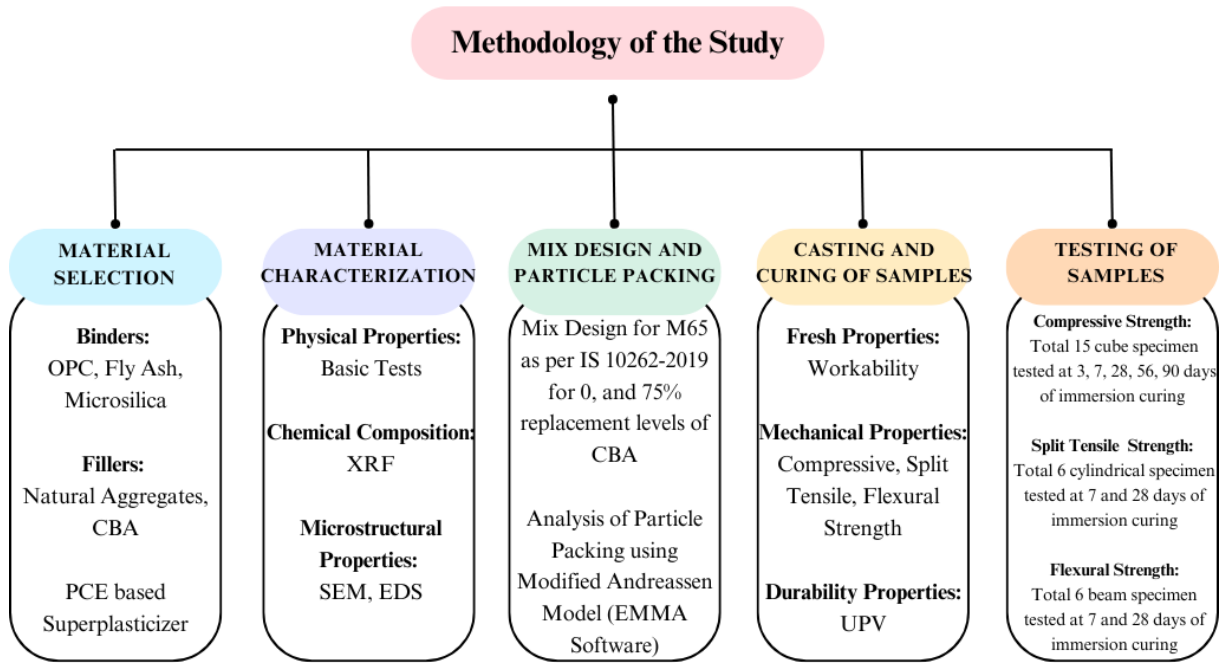


Figure 4. Methodology of the present study

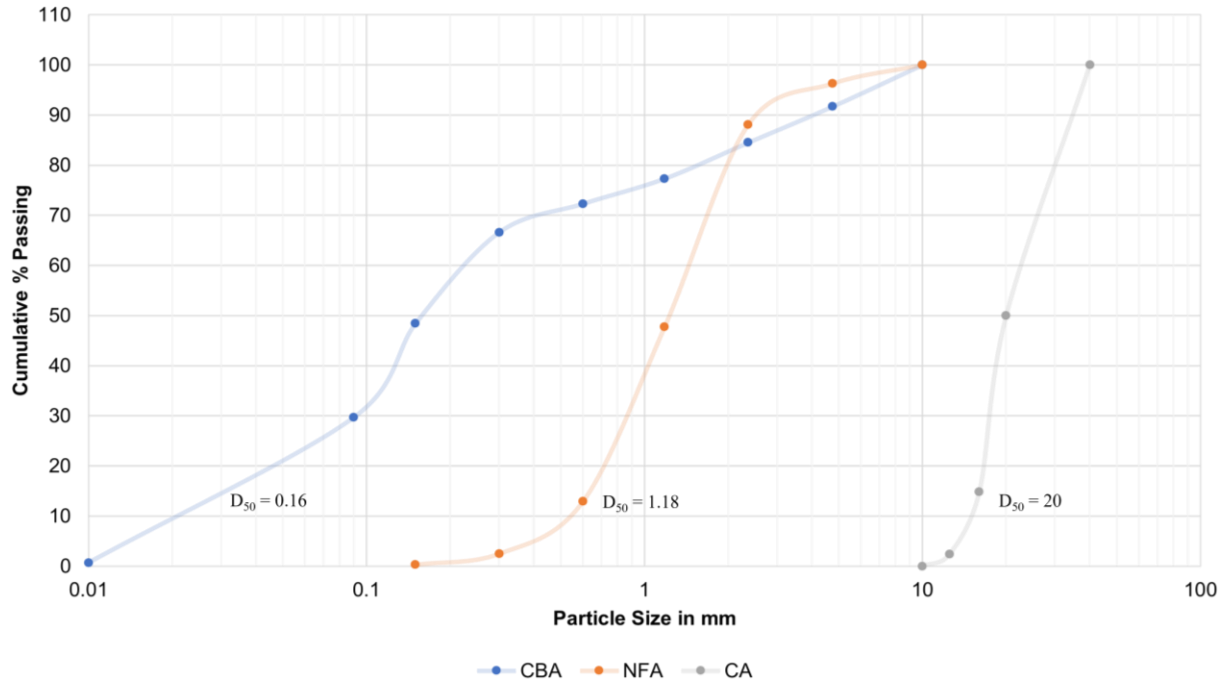


Figure 5. Particle Size Distribution of CA, NFA, and CBA

**Table 1.** Physical Properties of Materials

Material	Test	IS Code Reference	Results	Requirement	Conformity to IS Code
Cement	Fineness (90 $\mu$ )	[36]	5.66%	<10%	Yes
	Specific Surface	[37]	480.54 m <sup>2</sup> /kg	>225 m <sup>2</sup> /kg	Yes
	Consistency	[38]	25%	25 to 33%	Yes
	Specific Gravity	[39]	3		
	Initial Setting Time	[40]	80 mins	>30 mins	Yes
	Final Setting Time		230 mins	<600 mins	Yes
Compressive Strength			72 $\pm$ 1 hr: 39.5 MPa	27 MPa	Yes
		[41]	168 $\pm$ 2 hr: 45.5 MPa	37 MPa	Yes
			672 $\pm$ 4 hr: 53 MPa	53 MPa	Yes
Fly Ash	Fineness (45 $\mu$ )	[34]	12%	<34%	Yes
	Specific Surface	[42]	524.51 m <sup>2</sup> /kg	min 320 m <sup>2</sup> /kg	Yes
	Specific Gravity	[34]	2.19		
Pozzolanic Activity Index (PAI)	[34]				
Microsilica	Fineness (45 $\mu$ )	[34]	2.20%	<10%	Yes
	Specific Surface	[43]	6484.67 cm <sup>2</sup> /gm		
	Specific Gravity	[34]	2.25		
CA	Particle size distribution	[44]	MSA 16 mm		
	Specific Gravity	[45]	2.68		
	Water absorption	[45]	0.50%	<0.5%	Yes
NFA	Particle size distribution	[44]	Zone II		
	Specific Gravity	[45]	2.66		
	Water absorption	[45]	1%	<2%	Yes
	Silt content	[46]	1.25%		
CBA	Particle size distribution	[44]	Zone II		
	Specific Gravity	[45]	2.36		
	Water absorption	[45]	30%		
	Silt content	[46]	5%	<6%	Yes

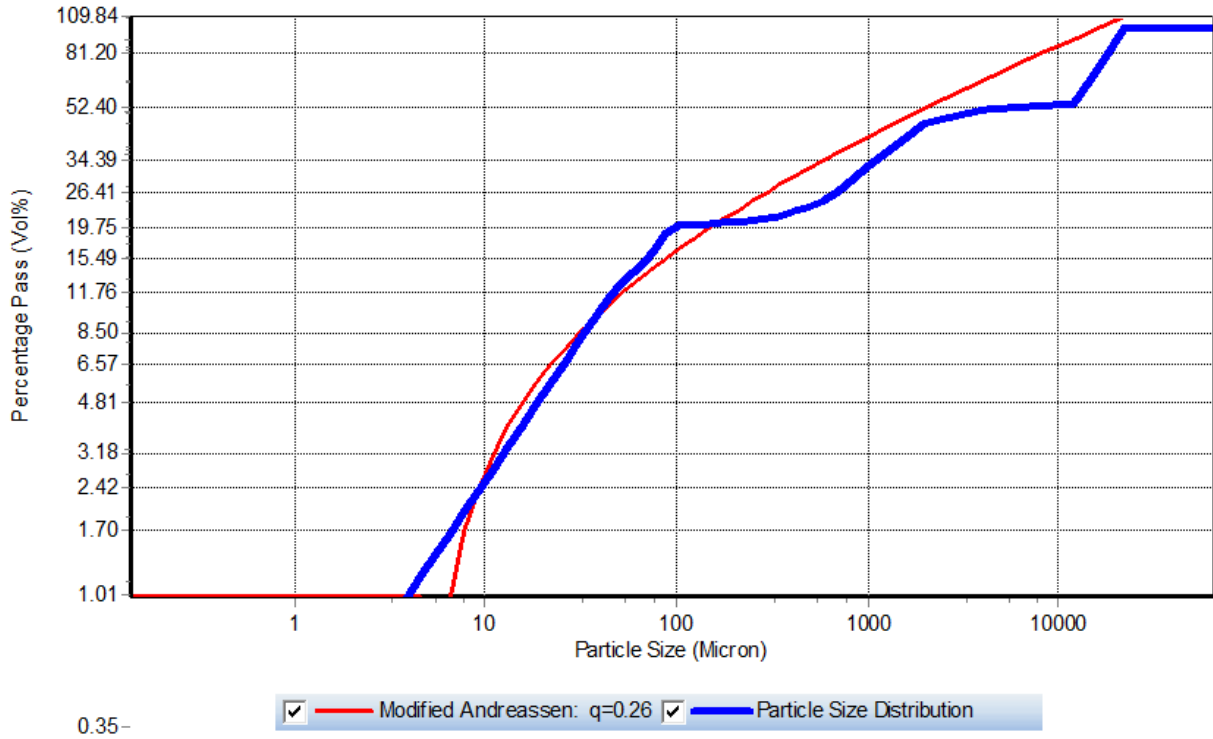
**Table 2.** Chemical Composition of Materials

Material	Component (% wt)										
	SiO <sub>2</sub>	Al <sub>2</sub> O <sub>3</sub>	Fe <sub>2</sub> O <sub>3</sub>	CaO	MgO	K <sub>2</sub> O	Na <sub>2</sub> O	SO <sub>3</sub>	P <sub>2</sub> O <sub>5</sub>	Mn <sub>2</sub> O <sub>3</sub>	TiO <sub>2</sub>
OPC	21.19	4.83	4.62	62.40	1.08	--	--	2.24	--	--	--
Fly Ash	62.27	20.65	5.48	3.04	0.69	1.26	0.08	0.10	0.02	0.06	1.40
Microsilica	90.25	0.65	0.7	0.55	0.75	1.45	0.7	0.35	--	--	--
CBA	54.66	21.85	6.86	4.45	0.58	1.04	0.16	0.17	0.31	0.06	1.47

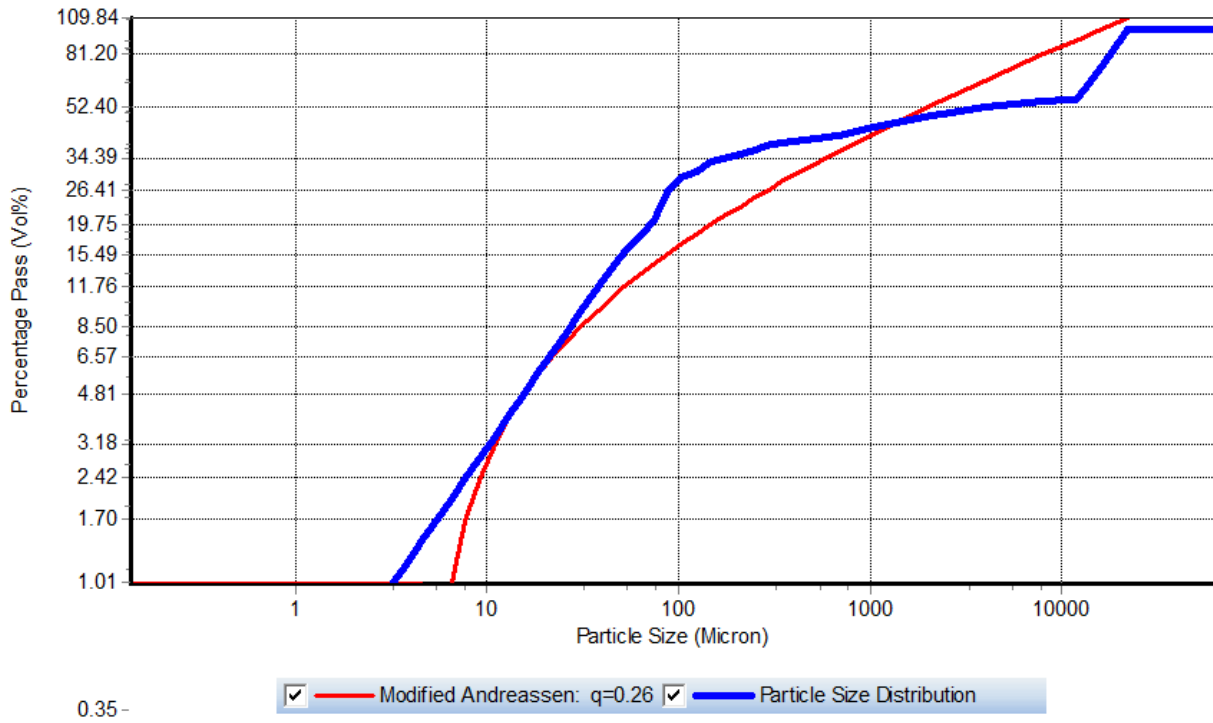
**Table 3.** Concrete Mix Proportion

Mix	CBA Replacement (%)	w/c <sub>m</sub>	kg/m <sup>3</sup>							
			Cement	Fly ash	Microsilica	NFA	CBA	CA	Water	PCE
CBA0	0	0.29	388.84	72.91	24.30	757	0	1044.51	141.57	3.88
CBA75	75	0.29	388.84	72.91	24.30	189.3	567.7	1044.51	141.57	3.88

Where CBA0 - control mix and CBA75 – concrete with CBA replacing 75% of NFA.



(a)



(b)

Figure 6. Particle Packing Curves for (a) CBA0 and (b) CBA75 Concrete

### 2.3. Testing Parameters

The microstructure of cement and fly ash mortar containing 80% OPC and 20% fly ash was studied using Scanning Electron Microscopy (SEM) to validate the results attained through experimental analysis at a curing age of 28 days. SEM combined with Energy-Dispersive X-ray Spectroscopy (EDS) was carried out to describe the elemental analysis of the mortar samples. The workability of concrete, in terms of slump, was evaluated as per procedures outlined in IS 1199 (Part 2)-2018 [48]. UPV tests were carried out on the 100 mm cube samples in accordance with IS 13311 (Part 1)-1992 [49]. UPV was performed to evaluate the quality and uniformity of the CBA concrete [18]. The higher the value of pulse velocity, the better the quality of the concrete [50]. The immersion-cured concrete samples were tested for compressive strength, flexural strength as per IS 516-1959 [51], and split tensile strength as per the procedures outlined in IS 5816-1999 [52]. The specimens were tested under a gradual uniform load without shock until failure.

### 2.4. Mixing, Casting and Curing of Samples

A 270 kg capacity horizontal shaft mixer was used to prepare the concrete mixes. Materials were introduced in the mixer sequentially as follows: initial mixing of coarse aggregates (CA) in sizes 16 mm and 12.5 mm along with NFA and CBA, followed by binders – cement, fly ash, and microsilica. The mixture of water and superplasticizer was introduced into the mix after obtaining a homogeneous dry mix. Each batch required approximately 10 to 12 minutes of mixing. Once prepared, the concrete was poured into a slump cone to measure its slump, then transferred into the pre-oiled moulds in three layers and vibrated for 20 to 30 seconds to ensure adequate compaction. After an initial period of 24 hours, the concrete specimens were demoulded and subsequently kept for immersion curing till the day of testing. Figure 7 represents the concrete specimens used for various tests.

### 2.5. Testing Methodology

#### 2.5.1. Compressive Strength

Cube specimens of 100×100×100 mm were cast to assess the compressive strength at 3, 7, 28, 56, and 90 days. Following the curing process, the specimens were cleaned to remove excess water and loose materials and placed on the Compression Testing Machine (CTM). The specimens were tested under a gradual uniform load of 140 kg/cm<sup>2</sup>/min until failure without shock.

#### 2.5.2. Split Tensile Strength

Cylinder specimens of size 150 mm diameter and 300 mm height were cast to assess the split tensile strength at 7 and 28 days. Before testing, the specimens were cleaned and placed on the CTM with the standard splitting apparatus. The specimens were tested under a gradual uniform load of 1.2–2.4 N/mm<sup>2</sup>/min without shock until failure.

#### 2.5.3. Flexural Strength

Beams of size 500×100×100 mm were cast to assess the flexural strength at 7 and 28 days of immersion curing. Before testing, the specimens were cleaned and placed on the flexural testing machine. The specimens were tested under a gradual uniform load of 7 kg/cm<sup>2</sup>/min without shock until failure.

#### 2.5.4. Ultrasonic Pulse Velocity (UPV)

Prior to the compressive strength test, UPV tests were conducted on the 100 mm cube samples. UPV was performed to evaluate the quality and uniformity of the CBA concrete. The higher the value of pulse velocity, the better the quality of the concrete. The pulse velocity can be determined using Equation (1).

$$V = \frac{L}{T} \quad (1)$$

Where V is the pulse velocity measured in km/s, L is the distance between the transducers, and T is the transit time in  $\mu$ s.

Table 4 represents the summary of the tests performed and the reference codes.

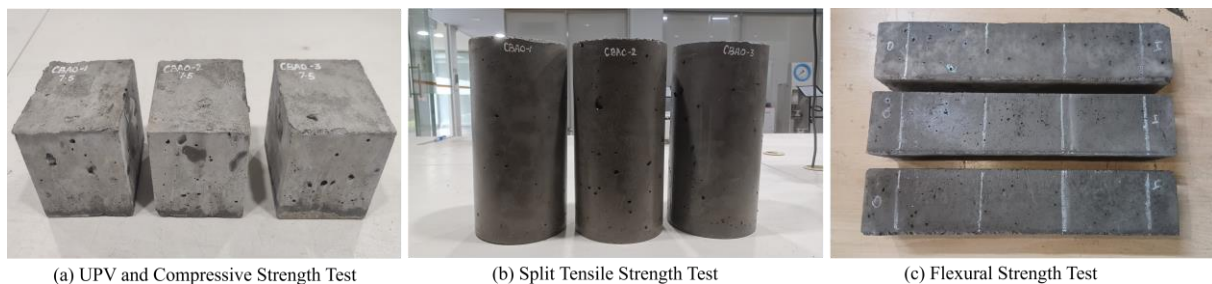


**Figure 7.** Concrete Specimens for Various Tests

**Table 4.** Details of Tests and Reference Codes

Test	Specimen	Curing age (days)	Dimensions (mm)	Total no. of Specimen	Loading Rate	Reference Code
Compressive Strength	Cube	3, 7, 28, 56, 90	100 × 100 × 100	15	140 kg/cm <sup>2</sup> /min	[51]
Flexural Strength	Beam	7, 28	500 × 100 × 100	6	7 kg/cm <sup>2</sup> /min	[51]
Split Tensile Strength	Cylinder	7, 28	150 $\phi$ × 300 h	6	1.2 - 2.4 N/mm <sup>2</sup> /min	[52]

$\phi$  – diameter and h – height

## 2.6. Morphology and Microstructural Analysis

SEM analysis was carried out at different locations at several magnifications. However, the results presented in this study are of 20 kx magnification. SEM combined with EDS was carried out for accelerated curing conditions to describe the elemental analysis of the various concrete samples and observe the morphological changes in the concrete.

## 3. Results and Discussion

### 3.1. Morphology and Microstructural Analysis

The hydration of silicates and calcium in binders leads to  $\text{Ca}(\text{OH})_2$  formation in the mortar mixes, initially evidenced by the presence of portlandite crystals. The SEM analysis showed prominent hexagonal portlandite crystals and the formation of dense and continuous CSH in fly ash mortar due to the pozzolanic reactions between fly ash, dicalcium, or tricalcium silicates in cement. This results in the formation of dense CSH during the later stages of hydration and pozzolanic reactions, contributing to the enhanced strength of fly ash blended mortar. The additional CSH from the pozzolanic reactions led to dense pore structures and higher strength gains at all ages [32].

Figure 8 and Figure 9 illustrate the SEM images and EDS spectrum of cement and fly ash mortar for accelerated curing conditions, respectively. Relatively, cement mortar depicts denser ettringite, whereas fly ash mortar exhibits a denser pore structure and  $\text{Ca}(\text{OH})_2$ . The EDS spectrum of cement and fly ash mortar indicates the presence of calcium, magnesium, aluminate, silicate, and hematite as the predominant oxide composition. Table 5 presents the chief oxides based on the atomic weight (%) obtained from EDS.

### 3.2. Fresh Properties

Figures 10 and 11 illustrate the slump patterns and slump values of the CBA0 and CBA75 mix, respectively. The results showed an increased slump with the addition of CBA in concrete, indicating increased workability in the concrete mixes, contradicting the results reported in [1, 53, 54]. Moreover, the observed increase in slump could be attributed to the higher water requirement due to the porous structure and higher water absorption of CBA in the mix. The incorporation of water absorption correction of CBA possibly led to the increased workability of the concrete mixes. Additionally, the slump showed a collapsed pattern, further exhibiting significant bleeding, segregation, and lower setting time, posing a significant challenge in incorporating CBA in concrete.

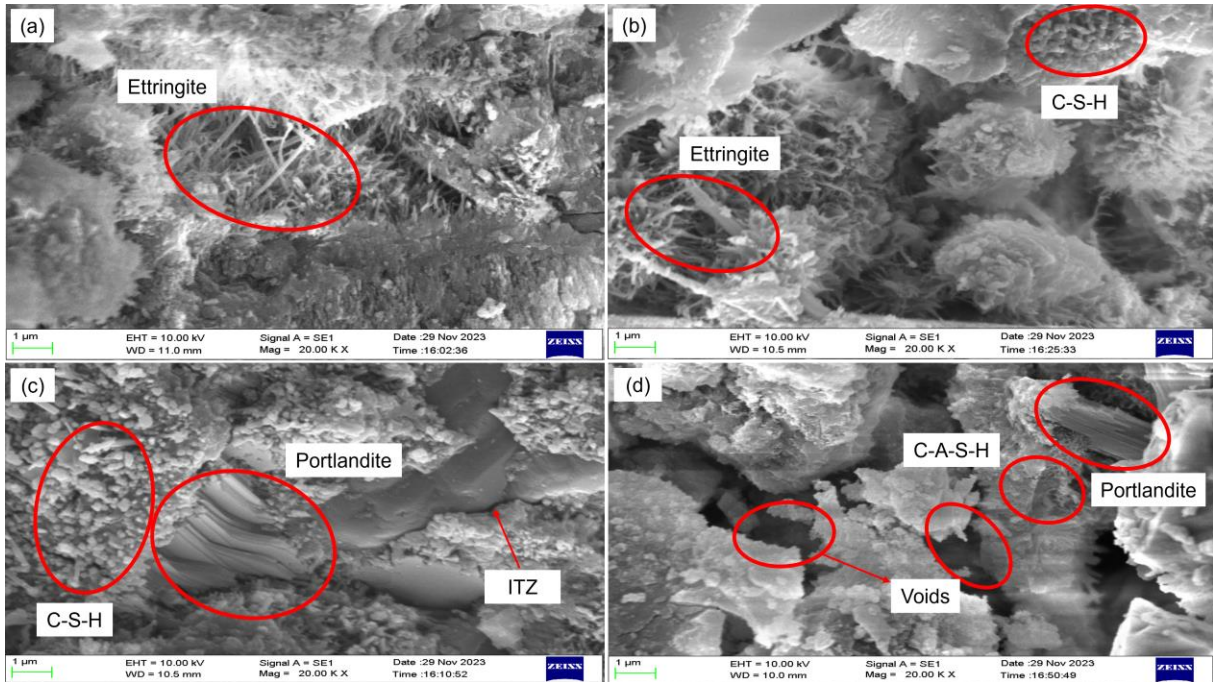


Figure 8. SEM Images of (a),(b) Cement Mortar and (c),(d) Fly Ash Mortar for Accelerated Curing

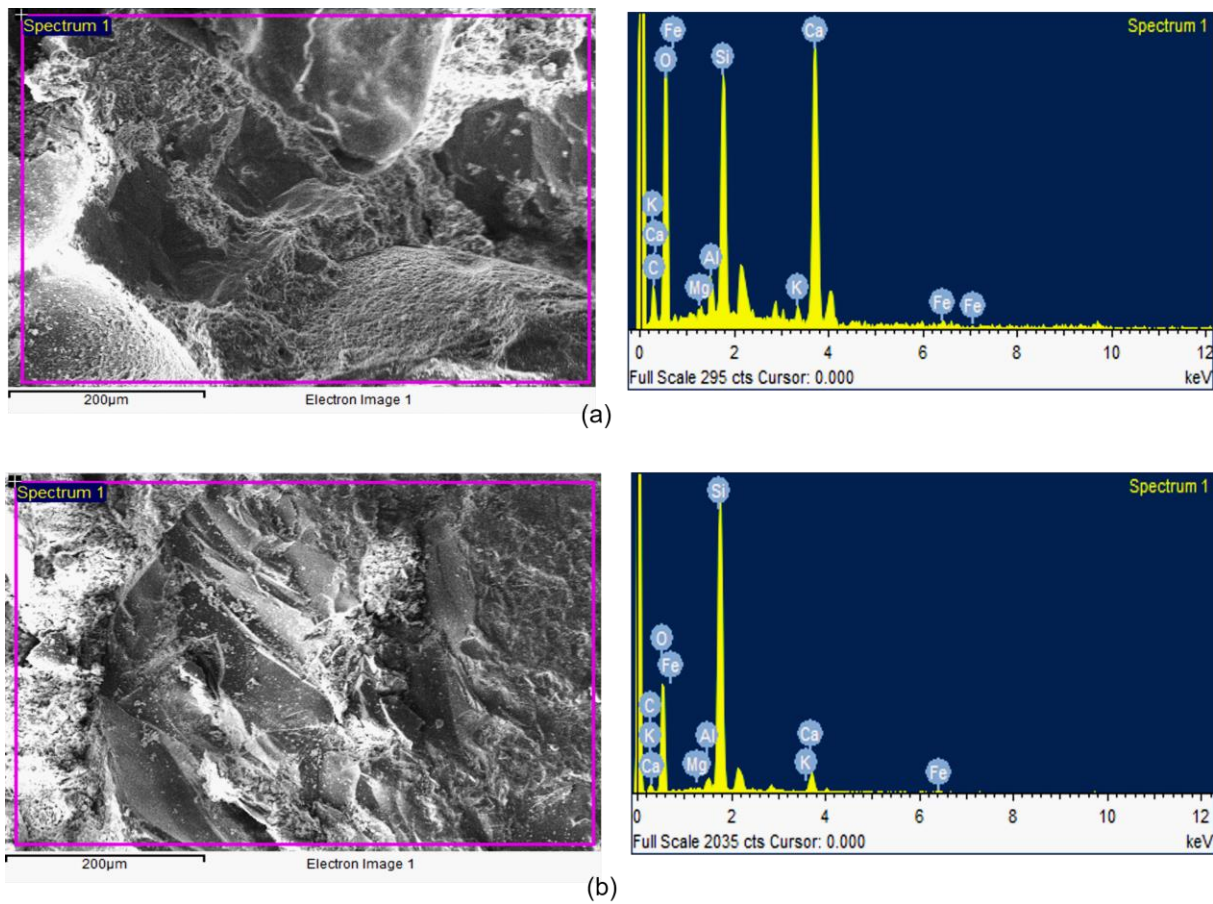
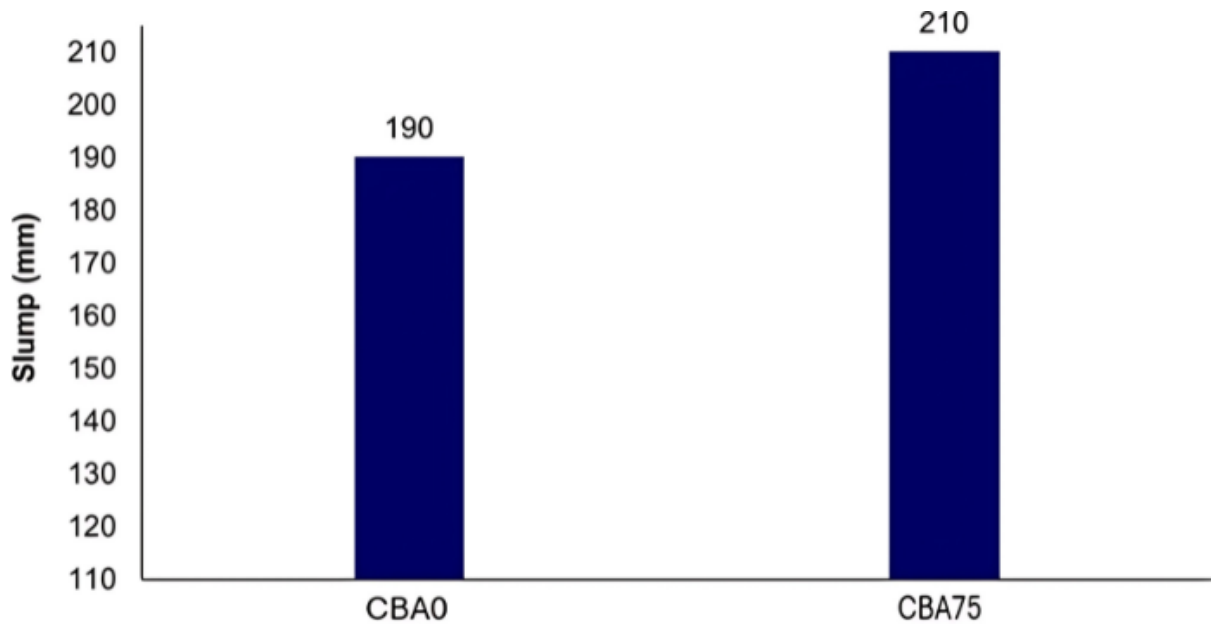


Figure 9. EDS Spectrum of (a) Cement Mortar and (b) Fly Ash Mortar

**Table 5.** Predominant Oxides present in Cement and Fly Ash Mortar

Mix Type	SiO <sub>2</sub>	Al <sub>2</sub> O <sub>3</sub>	Fe <sub>2</sub> O <sub>3</sub>	CaO	K <sub>2</sub> O	MgO
CM	10.27	1.52	1	25.67	0.83	0.48
FM	36.24	1.22	0.33	5.41	0.29	0.04

**Figure 10.** Slump Patterns of (a) CBA0 and (b) CBA75**Figure 11.** Slump Values of Concrete Mixes

### 3.3. Mechanical Properties

Table 6 summarizes the test results of the control and CBA concrete at various curing ages.

#### 3.3.1. Compressive Strength

All the concrete mixes attained the criteria of HSC. Compressive strength enhancement could be associated with the lower  $w/c_m$  ratio and particle packing. The inclusion of CBA in concrete significantly influenced the 28-day compressive strength. Figure 12 illustrates the trend of compressive strength of concrete mixes at different curing ages. CBA concrete initially exhibited lower compressive strength at 3 and 7 days, surpassing the strength of control concrete at 28, 56, and 90 days of curing.

The initial decrease in compressive strength could be attributed to the higher water requirement and porosity of CBA concrete. Relative to the control concrete, the compressive strength of CBA concrete decreased by 6.18% and 5.84% at 3 and 7 days and increased by 8.14%, 4.53%, and 2.97% at 28, 56, and 90 days, respectively. The increase in compressive strength of CBA concrete could be attributed to factors like reduced  $w/c_m$  ratio, improved particle packing, and the formation of secondary hydration products. This could be due to the pozzolanic activity of CBA, which initiates after 14 days and contributes to strength gain at later stages, with substantial consumption of calcium hydroxide becoming evident after 90 days. Over time, the initiation of pozzolanic properties of CBA causes

the pores to be filled with excess CSH produced through the pozzolanic reactions between CBA and  $\text{Ca}(\text{OH})_2$ . The microstructure of CBA concrete becomes dense, consequently increasing the compressive strength of CBA concrete at a higher rate than the control concrete [55]. Furthermore, incorporating (High Range Water Reducing Admixture) HWRA enhances the compressive strength of concrete blends, substituting CBA for NFA. This study utilized a 0.8% superplasticizer dosage for both the CBA0

and CBA75 mixes, potentially influencing the compressive strength of concrete samples. However, the rate of increase in compressive strength decreases with increasing curing period. The comparison finds the CBA mix to provide promising outcomes when 75% is used to substitute NFA in concrete. All the specimens exhibited a brittle failure when subjected to compressive stresses. Figure 13 represents the failure patterns of CBA0 and CBA75 under compressive stresses.

**Table 6.** Summary of Test Results

Test	Reference code	Results (MPa)	Requirements	Conformity to IS Code
<b>For CBA0</b>				
Compressive Strength	3 days [51]	41.92	40% of $f_{ck}=30$ MPa	Yes
	7 days	60.28	65% of $f_{ck}=48.7$ MPa	Yes
	28 days	73.73	65 MPa ( $f_{ck}$ )	Yes
	56 days	75		
	90 days	79.93		
Split Tensile Strength	7 days [52]	3.38	10% of compressive strength	Yes
	28 days	4.23		
Flexural Strength	7 days [51]	7.4		
	28 days	8.5	$0.7\sqrt{f_{ck}}=5.64$ MPa	Yes
<b>For CBA75</b>				
Compressive Strength	3 days [51]	39.33	40% of $f_{ck}=30$ MPa	Yes
	7 days	56.76	65% of $f_{ck}=48.7$ MPa	Yes
	28 days	79.73	65 MPa ( $f_{ck}$ )	
	56 days	78.4		
	90 days	82.3		
Split Tensile Strength	7 days [52]	3.04	10% of compressive strength	Yes
	28 days	3.25		
Flexural Strength	7 days [51]	5		
	28 days	7.2	$0.7\sqrt{f_{ck}}=5.64$ MPa	Yes

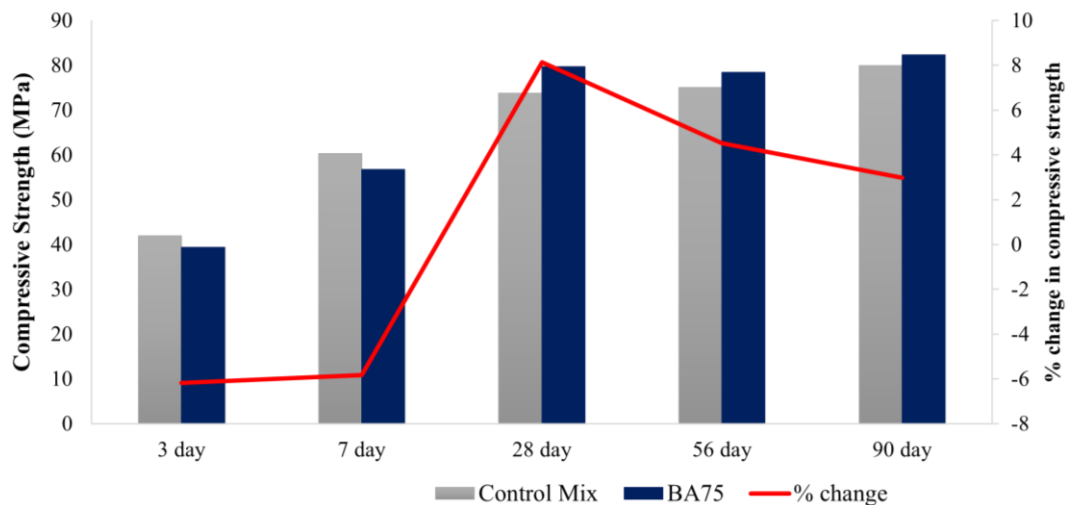


**Figure 12.** The trend of compressive strength of concrete at different curing ages



**Figure 13.** Failure Pattern of (a) CBA0 and (b) CBA75 under compressive stresses

### 3.3.2. Flexural Strength

The flexural strength increased with increasing curing ages for all the concrete specimens. However, CBA concrete exhibited lower flexural strength than control concrete. Figure 14 illustrates the trend of flexural strength of concrete at different curing ages. Relative to control concrete, the flexural strength of CBA concrete decreased by 32.43% and 15.29% at 7 and 28 days of curing, respectively. This reduction in flexural strength can be attributed to the increased porosity of the concrete caused by excessive CBA in the mix, enabling an easy propagation of cracks through them and due to the hindered pozzolanic activities [23]. This declining trend of flexural strength with CBA content aligns with the outcomes reported by previous studies on HSC [30]. Substituting weaker materials like CBA for sand partially or completely results in a weak paste and increased porosity, resulting in a larger ITZ, hindering the complete hydration of cement and consequently promoting microcrack propagation and interface fracture when subjected to stresses. Subsequently, this reduces the flexural strength of CBA concretes at higher replacement levels [55]. The specimens tested for flexure failed abruptly due to the rapid crack formation. Figure 15 represents the failure pattern of CBA0 and CBA75 when subjected to flexural stresses.

### 3.3.3. Split Tensile Strength

Figure 16 illustrates the trend of split tensile strength of concrete at different curing ages. The concrete specimens followed a similar declining trend for split tensile strength with substituting CBA in concrete. The test outcomes reveal that the incorporation of CBA in concrete enhanced the split tensile strength across all curing periods. However, the CBA concrete exhibited lower split tensile strength at 7-day and 28-day intervals compared to the control mix. The primary factors contributing to the decreased split

tensile strength in CBA concrete are increased porosity and pore distribution [55]. Compared to the control mix, the 7-day and 28-day split tensile strength of CBA concrete decreased by 10.06% and 23.17%, respectively. The decline in split tensile strength with increased CBA substitution levels is attributed to inadequate interlocking between aggregates and the weakened interfacial transition zone (ITZ) due to the porosity of CBA particles [29]. Additionally, the higher water absorption of CBA hinders concrete compaction, leading to weak bonding between aggregates and cementitious materials, thereby contributing to the reduced split tensile strength of CBA concretes [28]. Figure 17 represents the failure patterns of CBA0 and CBA75 under tensile stresses.

### 3.3.4. Ultrasonic Pulse Velocity

Table 7 summarizes the UPV results, and Figure 18 illustrates the UPV trend of concrete specimens at 7, 28, 56, and 90 days of curing. Aligning with the results obtained in previous studies [56], UPV increased with incorporating CBA in concrete. The UPV results of CBA concrete are comparable to control concrete at an early age, while there is a notable increase in UPV at 28, 56, and 90 days. In comparison to CBA0, the UPV values of the CBA75 mix increased by only 0.34% and 0.21% at 3 and 7 days of curing, respectively. However, CBA75 exhibited a significant increase of 12.23%, 27.61%, and 32.02% at a curing age of 28, 56, and 90 days, respectively. This increase in pulse velocity values could be due to the densification of the microstructure, as supported by the SEM images. Furthermore, the rate of increase in UPV values from 3 days to 28 days was higher for CBA75 than CBA0, ranging from 0.02 to 12.97% and 0.6 to 28.46% for CBA0 and CBA75, respectively. The quality of concrete can be classified as 'good' for all the concrete specimens and classified as 'excellent' for CBA concrete at later stages.

Towards a New Approach in Designing High-Strength Concrete:  
Challenges in Replacing Three-Fourth of Natural Fine Aggregate with Coal Bottom Ash

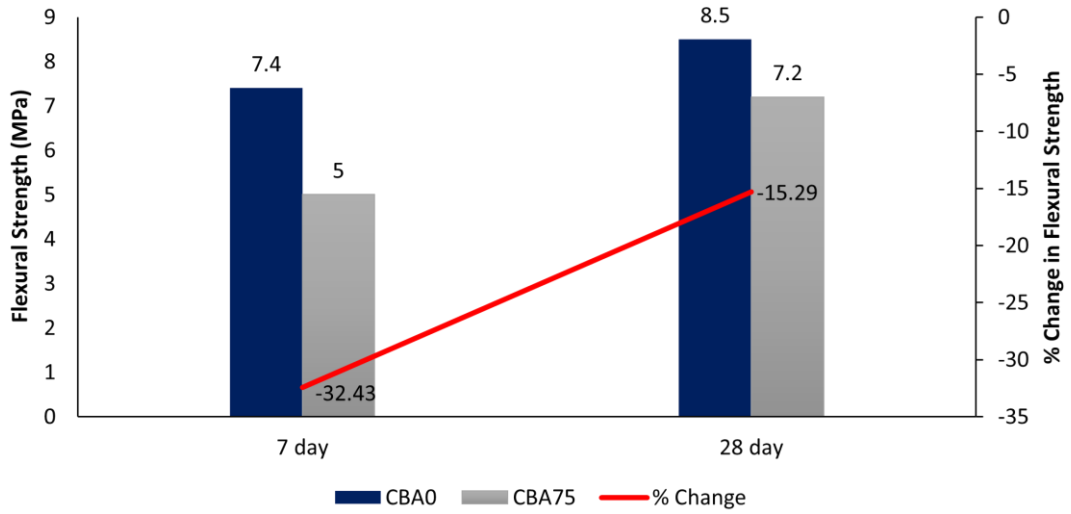


Figure 14. The trend of flexural strength of concrete at different curing ages



(a)

(b)

Figure 15. Failure Pattern of (a) CBA0 and (b) CBA75 under flexural stresses

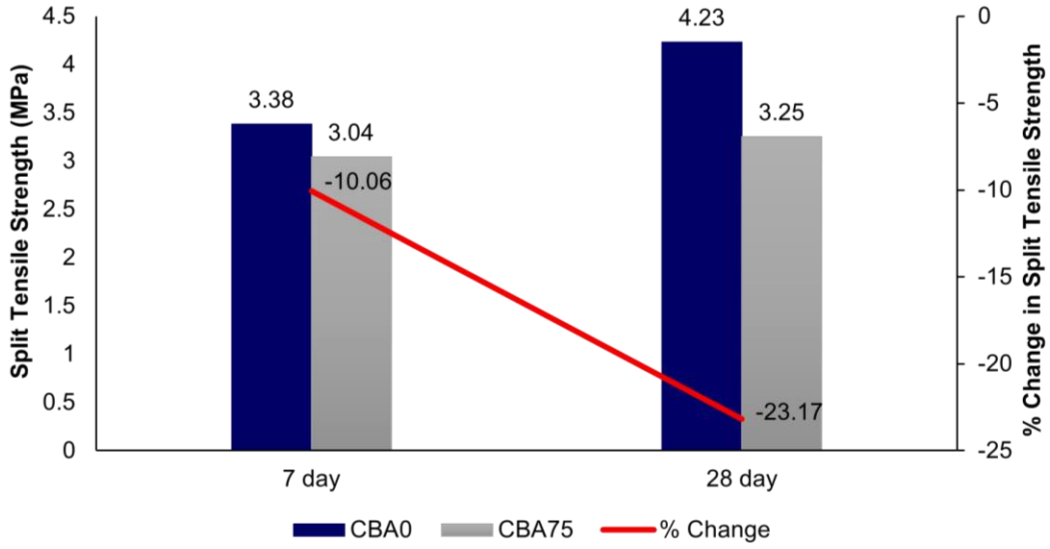


Figure 16. The trend of split tensile strength of concrete at different curing ages

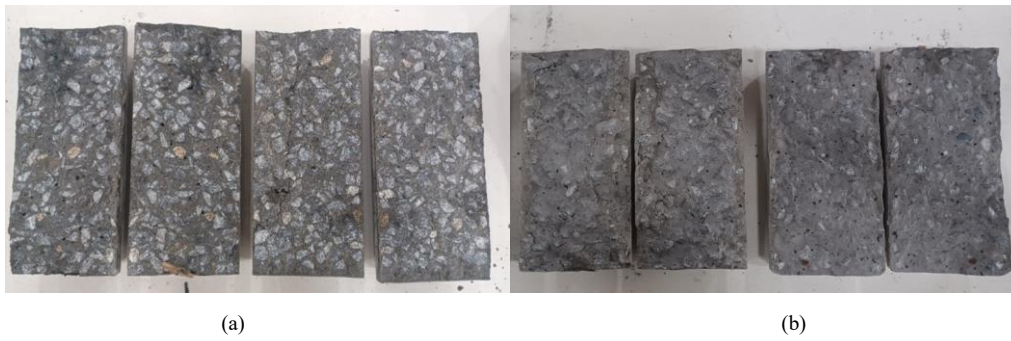


Figure 17. Failure Pattern of (a) CBA0 and (b) CBA75 under tensile stresses

Table 7. Results of UPV for Trial Concrete Mixes

Mix	Ultrasonic Pulse Velocity (m/s)					Concrete Grading
	3 days	7 days	28 days	56 days	90 days	
CBA0	3498	3524	3623	4093	4094	Good
CBA75	3510	3531	4066	5223	5405	Good to Excellent

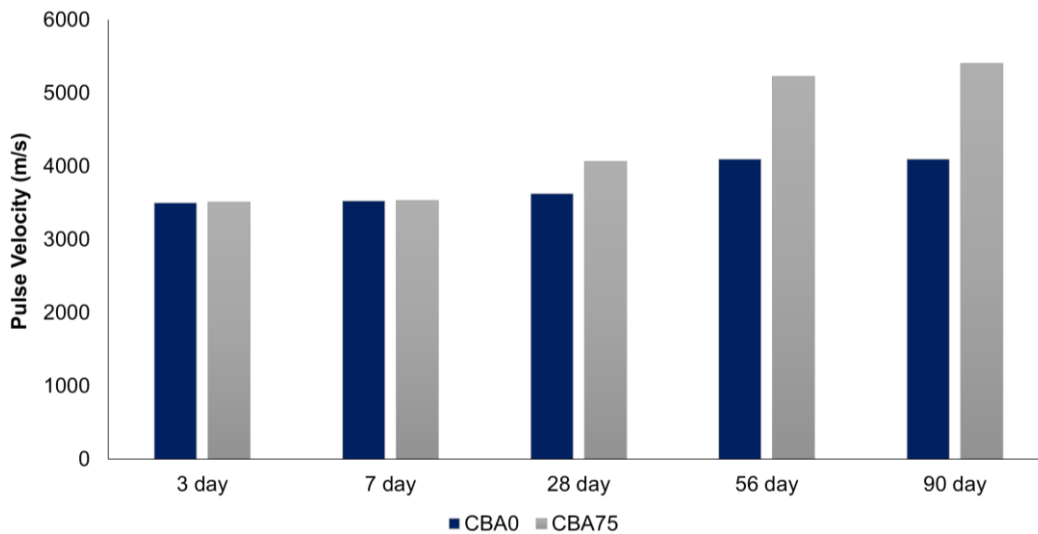


Figure 18. The trend of UPV of concrete at different curing ages

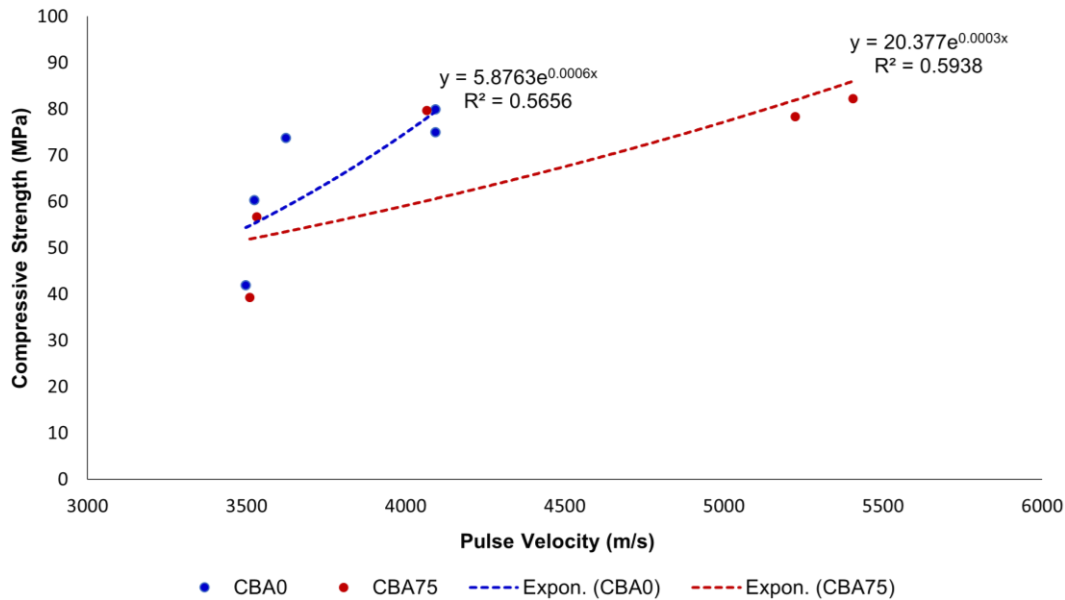


Figure 19. Relationship between Compressive Strength and Pulse Velocity of Concrete

#### 4. Relationship between Compressive Strength and UPV

Figure 19 shows the correlation between pulse velocity and compressive strength of concrete. The observed relationship indicates that compressive strength increases with higher pulse velocity values, demonstrating a positive correlation between UPV and compressive strength. A study by M. Singh, supports this correlation, reporting  $R^2$  values between 0.59 and 0.85 [55]. The equations representing the relationship of CBA0 and CBA75 are given as equations (2) and (3), respectively. The regression analysis shows an  $R^2$  value of 0.56 to 0.59, indicating a moderate correlation between pulse velocity and concrete compressive strength. The coefficient of determination surpassing 0.7 highlights a significant relationship between the variables [55].

$$\text{CBA0 } C = 5.8763e^{0.0006V}; R^2 = 0.5656 \quad (2)$$

$$\text{CBA75 } C = 20.377e^{0.0003V}; R^2 = 0.5938 \quad (3)$$

Where  $C$  = Compressive strength of concrete,  $V$  = Pulse velocity, and  $R^2$  represents the coefficient of determination.

#### 5. Challenges in Utilizing CBA in Concrete

Figure 20 depicts the results of the flow table test conducted on mortar mixes incorporating CBA at substitution levels of 0 and 75%, assessing the bleeding tendencies of these CBA mixes. The flow characteristics of

mortar mixes were observed to increase as CBA replacement increased. This trend could be attributed to a greater tendency of bleeding at higher levels of CBA replacement. This trend aligns with the previous studies by Andrade et al. [57]. However, these results contradict the findings reported by M. Singh & Siddique [2, 12]. The increased bleeding could be attributed to the increased demand for water in the mix due to the higher absorption of CBA. It is evident that the increase in water content substantially affects the outcomes. However, the rate at which water is released from CBA plays a vital role in the escalation of bleeding in the mix [57]. Incorporating CBA in concrete poses several challenges, particularly concerning excessive bleeding. This issue becomes more pronounced with increasing CBA content in concrete, leading to potential durability concerns. Thus, addressing bleeding is crucial to ensure the durability of concrete. Optimizing binder content and adjusting the mix proportions can effectively control bleeding while ensuring the desired workability and strength. Figure 21 illustrates a fishbone diagram for the factors affecting the bleeding and segregation in the concrete mix.



Figure 20. Spread of Flow Table Test for Mortar Mixes incorporating CBA at replacement levels of (a) 0% and (b) 75%

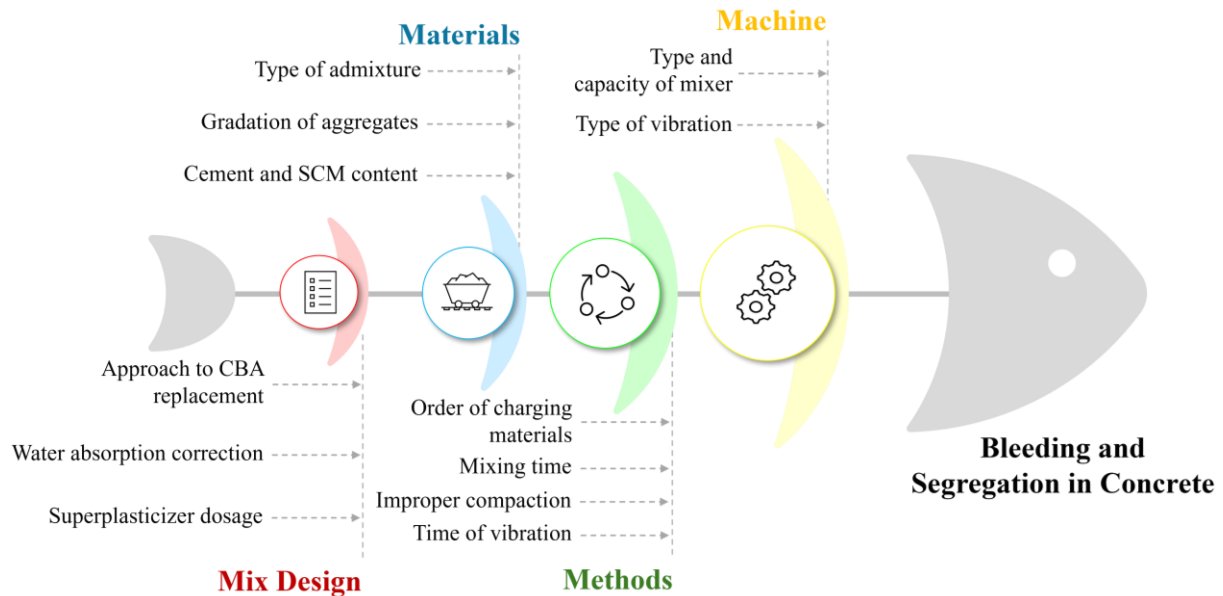


Figure 21. Fishbone Diagram for the Factors Affecting the Bleeding and Segregation of Concrete

## 6. Conclusions

This study demonstrates the potential of using a ternary blend of OPC, fly ash, and silica fumes, combined with coarse and fine CBA, to develop HSC with reduced reliance on natural sand. By achieving HSC-grade compressive strength with a lower  $w/c_m$  ratio and addressing workability challenges, the findings provide valuable insights for optimizing sustainable concrete mixes. This research offers a foundation for future studies seeking to balance strength, durability, and workability in advanced concrete applications. This article presents an experimental investigation of the influence of HVCBA, incorporating 75% CBA on the mechanical properties of HSC. The following conclusions can be drawn from the experimental investigation of replacing NFA with a high volume of CBA in the designed mix:

- The inclusion of high-volume CBA in concrete significantly influences its compressive strength, showing an initial decrease but a substantial increase at later curing stages. The improved performance can be attributed to factors such as reduced  $w/c_m$  ratio, enhanced particle packing, and the pozzolanic activity of CBA, which contribute to strength gain over time. The findings suggest that substituting 75% of NFA with CBA yields promising results in terms of strength.
- Though the flexural strength increased with increasing curing age, CBA concrete mixes exhibited weaker performance, showing a significant reduction of 32.43% and 15.29% at 7 and 28 days, respectively, attributed to higher porosity and hindered pozzolanic activity at early ages.
- CBA in concrete led to a consistent decline in split tensile strength, with CBA concrete exhibiting a

reduction of 10.06% and 23.17%, respectively, at 7 and 28 days of curing. This could be due to the weakened aggregate-binder bond resulting from the higher requirement of water in the CBA mix, which leads to increased porosity and ultimately results in reduced tensile strength of the concrete specimen.

- Incorporating CBA in concrete enhances UPV, signifying improved microstructure densification. Initially comparable to the control mix, UPV values for CBA concrete notably increase at 56 and 90 days, indicating 'good' quality at early curing ages and 'excellent' quality at later stages for all specimens.
- The graph of the UPV and the compressive strength of concrete confirm a moderate correlation, with  $R^2$  values of 0.56 to 0.59, supporting previous findings ( $R^2 = 0.59$  to 0.85).
- The incorporation of fly ash in mortar enhances strength through pozzolanic reactions, forming dense CSH and reducing porosity. SEM analysis confirms dense pore structures and prominent portlandite crystals. This underscores the role of fly ash in improving mortar durability and strength through advanced hydration processes.
- CBA in concrete introduces challenges, particularly excessive bleeding, resulting from higher CBA content. Addressing bleeding is crucial, necessitating the optimization of binder content and mix proportions to maintain desired workability and strength while mitigating durability concerns.

## Acknowledgements

The authors credit UPCL, Karnataka, India, for supplying fly ash and coal bottom ash and Ramco Cements

Ltd. for supplying cement. Acknowledgements to Shivam Kumar, Vansh Vardhan, and Kiran Choudhary, B.Tech (Civil Engineering), for their support during the experimental works.

## REFERENCES

- [1] G. Singh and ShriRam, "Microstructural and other properties of copper slag-coal bottom ash incorporated concrete using fly ash as cement replacement," *Innovative Infrastructure Solutions*, vol. 8, no. 2, pp. 1–13, Feb. 2023, doi: 10.1007/s41062-023-01051-7.
- [2] M. Singh and R. Siddique, "Strength properties and micro-structural properties of concrete containing coal bottom ash as partial replacement of fine aggregate," *Constr Build Mater*, vol. 50, pp. 246–256, 2014, doi: 10.1016/j.conbuildmat.2013.09.026.
- [3] L. Kudva P. and R. M. Suralikerimath, "Effect of Supplementary Cementitious Materials on Mechanical Properties and Thermal Conductivity of Concretes and Masonry Blocks," 2018, pp. 531–541. [Online]. Available: <http://www.springer.com/series/15087>
- [4] T. Ali *et al.*, "Investigation on Mechanical and Durability Properties of Concrete Mixed with Silica Fume as Cementitious Material and Coal Bottom Ash as Fine Aggregate Replacement Material," *Buildings*, vol. 12, no. 1, pp. 1–14, Jan. 2022, doi: 10.3390/buildings12010044.
- [5] D. N. Nathe and Y. D. Patil, "Performance of coal bottom ash concrete at elevated temperatures," *Mater Today Proc*, vol. 65, pp. 883–888, Jan. 2022, doi: 10.1016/j.matpr.2022.03.519.
- [6] M. Rafieizonooz *et al.*, "Toxicity characteristics and durability of concrete containing coal ash as substitute for cement and river sand," *Constr Build Mater*, vol. 143, pp. 234–246, Jul. 2017, doi: 10.1016/j.conbuildmat.2017.03.151.
- [7] H. Alghamdi, "A review of cementitious alternatives within the development of environmental sustainability associated with cement replacement," *Environmental Science and Pollution Research*, vol. 29, no. 28, pp. 42433–42451, Jun. 2022, doi: 10.1007/s11356-022-19893-6.
- [8] Debasree, A. Amrin, D. R. Biswal, K. K. Sahoo, and P. K. Dhir, "Utilization of Bottom Ash and Pond Ash as a Partial Replacement for Sand in Cement Mortar and Concrete: A Critical Review," *Practice Periodical on Structural Design and Construction*, vol. 28, no. 4, pp. 1–17, Nov. 2023, doi: 10.1061/ppscfx.sceng-1325.
- [9] M. Rafieizonooz, E. Khankhaje, and S. Rezanian, "Assessment of environmental and chemical properties of coal ashes including fly ash and bottom ash, and coal ash concrete," *Journal of Building Engineering*, vol. 49, pp. 1–10, May 2022, doi: 10.1016/j.jobbe.2022.104040.
- [10] P. Laxman Kudva, G. Nayak, K. K. Shetty, and H. K. Sugandhini, "A sustainable approach to designing high volume fly ash concretes," in *Materials Today: Proceedings*, Elsevier Ltd, Jan. 2022, pp. 1138–1145. doi: 10.1016/j.matpr.2022.04.165.
- [11] L. Kudva P., G. Nayak, K. K. Shetty, and S. H.K., "Assessment of flexural response of RC beams and unrestrained shrinkage of fiber-reinforced high-volume fly ash-based no-aggregate concrete and self-compacting concrete," *Constr Build Mater*, vol. 431, Jun. 2024, doi: 10.1016/j.conbuildmat.2024.136527.
- [12] M. Singh and R. Siddique, "Effect of coal bottom ash as partial replacement of sand on workability and strength properties of concrete," *J Clean Prod*, vol. 112, pp. 620–630, Jan. 2016, doi: 10.1016/j.jclepro.2015.08.001.
- [13] C. Argiz, M. Á. Sanjuán, and E. Menéndez, "Coal Bottom Ash for Portland Cement Production," *Advances in Materials Science and Engineering*, pp. 1–7, 2017, doi: 10.1155/2017/6068286.
- [14] S. Kumar, K. Kapoor, S. P. Singh, P. Singh, and V. Sharma, "A review on the properties of natural and recycled coarse aggregates concrete made with different coal ashes," *Cleaner Materials*, vol. 5, pp. 1–29, Sep. 2022, doi: 10.1016/j.clema.2022.100109.
- [15] H. Hamada, A. Alattar, B. Tayeh, F. Yahaya, and A. Adesina, "Sustainable application of coal bottom ash as fine aggregates in concrete: A comprehensive review," *Case Studies in Construction Materials*, vol. 16, pp. 1–17, Jun. 2022, doi: 10.1016/j.cscm.2022.e01109.
- [16] N. Seav, K. S. Kim, J. H. Kim, S. W. Lee, and Y. K. Kim, "Effects of Roller Compacted Concrete Incorporating Coal Bottom Ash as a Fine Aggregate Replacement," *Sustainability (Switzerland)*, vol. 15, no. 14, pp. 1–21, Jul. 2023, doi: 10.3390/su151411420.
- [17] J. Seo, J. E. Kim, S. M. Jeon, S. Park, and H. K. Kim, "On guidelines for mix proportioning of concrete incorporating coal bottom ash as fine aggregate," *Materials and Structures/Materiaux et Constructions*, vol. 56, no. 7, pp. 1–15, Sep. 2023, doi: 10.1617/s11527-023-02205-w.
- [18] I. H. Yang, J. Park, N. Dinh Le, and S. Jung, "Strength Properties of High-Strength Concrete Containing Coal Bottom Ash as a Replacement of Aggregates," *Advances in Materials Science and Engineering*, vol. 2020, pp. 1–12, 2020, doi: 10.1155/2020/4246396.
- [19] S. A. Mangi, M. H. W. Ibrahim, N. Jamaluddin, M. F. Arshad, and S. W. Mudjanarko, "Recycling of coal ash in concrete as a partial cementitious resource," *Resources*, vol. 8, no. 2, pp. 1–10, Jun. 2019, doi: 10.3390/resources8020099.
- [20] N. Singh, B. Sharma, and M. Rathee, "Carbonation resistance of blended mortars and industrial by-products: A brief review," *Cleaner Materials*, vol. 4, pp. 1–18, Jun. 2022, doi: 10.1016/j.clema.2022.100058.
- [21] K. Muthusamy, M. H. Rasid, G. A. Jokhio, A. Mokhtar Albshir Budiea, M. W. Hussin, and J. Mirza, "Coal bottom ash as sand replacement in concrete: A review," *Constr Build Mater*, vol. 236, pp. 1–12, Mar. 2020, doi: 10.1016/j.conbuildmat.2019.117507.
- [22] W. Wongkeo and A. Chaipanich, "Compressive strength, microstructure and thermal analysis of autoclaved and air cured structural lightweight concrete made with coal bottom ash and silica fume," *Materials Science and Engineering A*, vol. 527, pp. 16–17, pp. 3676–3684, Jun. 2010, doi: 10.1016/j.msea.2010.01.089.

- [23] A. M. Hasim, K. A. Shahid, N. F. Ariffin, N. N. Nasrudin, and M. N. S. Zaimi, "Study on mechanical properties of concrete inclusion of high-volume coal bottom ash with the addition of fly ash," in *Materials Today: Proceedings*, Elsevier Ltd, 2021, pp. 1355–1361. doi: 10.1016/j.matpr.2021.11.400.
- [24] S. K. Goudar, K. N. Shivaprasad, and B. B. Das, "Mechanical properties of fiber-reinforced concrete using coal-bottom ash as replacement of fine aggregate," in *Lecture Notes in Civil Engineering*, vol. 25, Springer, 2019, pp. 863–872. doi: 10.1007/978-981-13-3317-0\_77.
- [25] S. Gooi, A. A. Mousa, and D. Kong, "A critical review and gap analysis on the use of coal bottom ash as a substitute constituent in concrete," *J Clean Prod*, vol. 268, pp. 1–26, Sep. 2020, doi: 10.1016/j.jclepro.2020.121752.
- [26] H. Zhou *et al.*, "Towards sustainable coal industry: Turning coal bottom ash into wealth," *Science of the Total Environment*, vol. 804, pp. 1–15, Jan. 2022, doi: 10.1016/j.scitotenv.2021.149985.
- [27] K. Tamanna, S. N. Raman, M. Jamil, and R. Hamid, "Coal bottom ash as supplementary material for sustainable construction: A comprehensive review," *Constr Build Mater*, vol. 389, pp. 1–19, Jul. 2023, doi: 10.1016/j.conbuildmat.2023.131679.
- [28] A. M. Hasim, K. A. Shahid, N. F. Ariffin, N. N. Nasrudin, and M. N. S. Zaimi, "Properties of high volume coal bottom ash in concrete production," in *Materials Today: Proceedings*, Elsevier Ltd, 2021, pp. 1861–1867. doi: 10.1016/j.matpr.2021.09.250.
- [29] N. Ankur and N. Singh, "Performance of cement mortars and concretes containing coal bottom ash: A comprehensive review," *Renewable and Sustainable Energy Reviews*, vol. 149, pp. 1–29, Oct. 2021, doi: 10.1016/j.rser.2021.111361.
- [30] H. K. Kim and H. K. Lee, "Use of power plant bottom ash as fine and coarse aggregates in high-strength concrete," *Constr Build Mater*, vol. 25, no. 2, pp. 1115–1122, Feb. 2011, doi: 10.1016/j.conbuildmat.2010.06.065.
- [31] Y. Luna, C. G. Arenas, A. Cornejo, C. Leiva, L. F. Vilches, and C. Fernández-Pereira, "Recycling by-products from coal-fired power stations into different construction materials," *International Journal of Energy and Environmental Engineering*, vol. 5, no. 4, pp. 387–397, Dec. 2014, doi: 10.1007/s40095-014-0120-6.
- [32] H. Ganesan, A. Sachdeva, P. Petrounias, P. Lampropoulou, P. K. Sharma, and A. Kumar, "Impact of Fine Slag Aggregates on the Final Durability of Coal Bottom Ash to Produce Sustainable Concrete," *Sustainability (Switzerland)*, vol. 15, no. 7, pp. 1–31, Apr. 2023, doi: 10.3390/su15076076.
- [33] "IS 269, Ordinary Portland Cement - Specifications," New Delhi, India: Bureau of Indian Standards, 2015, pp. 1–14.
- [34] "IS 1727, Methods of Test for Pozzolanic Materials," New Delhi, India: Bureau of Indian Standards, 1967, pp. 1–55.
- [35] "IS 383, Coarse and Fine Aggregate for Concrete," New Delhi, India: Bureau of Indian Standards, 2016, pp. 1–24.
- [36] "IS 4031 (Part 1), Method of Physical Tests for Hydraulic Cement; Part 1: Determination of Fineness by Dry Sieving," Reaffirmed 2016., New Delhi, India: Bureau of Indian Standards, 1996, pp. 1–7.
- [37] "IS 4031 (Part 2), Methods of Physical Tests for Hydraulic Cement; Part 2: Determination of Fineness by Blaine Air Permeability Method," Reaffirmed 2004., New Delhi, India: Bureau of Indian Standards, 1999, pp. 1–13.
- [38] "IS 4031 (Part 4), Methods of Physical Tests for Hydraulic Cement; Part 4: Determination of Consistency of Standard Cement Paste," Reaffirmed 2019., New Delhi, India: Bureau of Indian Standards, 1988, pp. 1–4.
- [39] "IS 4031 (Part 11), Methods of Physical Tests for Hydraulic Cement; Part 11: Determination Of Density," New Delhi, India: Bureau Of Indian Standards, 1988, pp. 1–6.
- [40] "IS 4031 (Part 5), Methods of Physical Tests for Hydraulic Cement; Part 5: Determination of Initial and Final Setting Times," New Delhi, India: Bureau of Indian Standards, 1988, pp. 1–5.
- [41] "IS 4031 (Part 6), Methods of Physical Tests for Hydraulic Cement; Part 6: Determination of Initial and Final Setting Times," Reaffirmed 2019., New Delhi, India: Bureau of Indian Standards, 1988, pp. 1–9.
- [42] "IS 3812 (Part 1), Pulverized Fuel Ash — Specification; Part 1: For Use as Pozzolana in Cement, Cement Mortar and Concrete," New Delhi, India: Bureau of Indian Standards, 2013, pp. 1–18.
- [43] "IS 15388, Silica Fume — Specification," New Delhi, India: Bureau of Indian Standards, 2003, pp. 1–13.
- [44] "IS 2386 (Part 1), Methods of Test for Aggregates for Concrete; Part 1: Particle Size and Shape," Reaffirmed 2016., New Delhi, India: Bureau of Indian Standards, 1963, pp. 1–23.
- [45] "IS 2386 (Part 3), Methods of Test for Aggregates for Concrete; Part 3: Specific Gravity, Density, Voids, Absorption and Bulking," Reaffirmed 2016., New Delhi, India: Bureau of Indian Standards, 1963, pp. 1–22.
- [46] "IS 2386 (Part 2), Methods of Test for Aggregates for Concrete; Part 2: Estimation of Deleterious Materials and Organic Impurities," New Delhi, India: Bureau of Indian Standards, 1963, pp. 1–21.
- [47] "IS 10262, Concrete Mix Proportioning - Guidelines," New Delhi, India: Bureau of Indian Standards, 2019, pp. 1–36.
- [48] "IS 1199 (Part 2), Fresh Concrete - Methods of Sampling, Testing and Analysis; Part 2: Determination of Consistency of Fresh Concrete," New Delhi, India: Bureau of Indian Standards, 2018, pp. 1–49.
- [49] "IS 13311 (Part 1), Non-Destructive Testing of Concrete - Methods of Test; Part 1: Ultrasonic Pulse Velocity," Reaffirmed 2004., New Delhi, India: Bureau of Indian Standards, 1992, pp. 1–14.
- [50] L. P. Kudva, G. Nayak, K. K. Shetty, and H. K. Sugandhini, "Mechanical Properties of Fiber-Reinforced High-Volume Fly-Ash-Based Cement Composite—A Long-Term Study," *Sustainability (Switzerland)*, vol. 15, no. 17, pp. 1–20, Sep. 2023, doi: 10.3390/su151713128.
- [51] "IS 516, Methods of Tests for Strength Of Concrete," New Delhi, India: Bureau of Indian Standards, 1959, pp. 1–25.
- [52] "IS 5816, Splitting Tensile Strength of Concrete - Method

- of Test,” New Delhi, India: Bureau of Indian Standards, 1999, pp. 1–11.
- [53] E. Aydin, “Novel coal bottom ash waste composites for sustainable construction,” *Constr Build Mater*, vol. 124, pp. 582–588, Oct. 2016, doi: 10.1016/j.conbuildmat.2016.07.142.
- [54] P. Khongpermguson *et al.*, “The mechanical properties and heat development behavior of high strength concrete containing high fineness coal bottom ash as a pozzolanic binder,” *Constr Build Mater*, vol. 253, pp. 1–9, Aug. 2020, doi: 10.1016/j.conbuildmat.2020.119239.
- [55] M. Singh, “Coal bottom ash,” in *Waste and Supplementary Cementitious Materials in Concrete: Characterisation, Properties and Applications*, Elsevier, 2018, pp. 3–50. doi: 10.1016/B978-0-08-102156-9.00001-8.
- [56] A. Saxena, S. S. Sulaiman, M. Shariq, and M. A. Ansari, “Experimental and analytical investigation of concrete properties made with recycled coarse aggregate and bottom ash,” *Innovative Infrastructure Solutions*, vol. 8, no. 7, pp. 1–18, Jul. 2023, doi: 10.1007/s41062-023-01165-y.
- [57] L. B. Andrade, J. C. Rocha, and M. Cheriaf, “Influence of coal bottom ash as fine aggregate on fresh properties of concrete,” *Constr Build Mater*, vol. 23, no. 2, pp. 609–614, Feb. 2009, doi: 10.1016/j.conbuildmat.2008.05.003.